

Author's response – "A representative density profile for the North Greenland snowpack"

Christoph Florian Schaller¹, Johannes Freitag¹, Sepp Kipfstuhl¹, Thomas Laepple², Hans Christian Steen-Larsen³, and Olaf Eisen^{1,4}

¹Alfred Wegener Institute, Helmholtz Centre for Polar and Marine Research, Bremerhaven, Germany

²Alfred Wegener Institute, Helmholtz Centre for Polar and Marine Research, Potsdam, Germany

³Centre for Ice and Climate, Niels Bohr Institute, University of Copenhagen, Denmark

⁴Department of Geosciences, University of Bremen, Germany

Correspondence to: Christoph Schaller (christoph.schaller@awi.de)

We would like to thank the two anonymous referees for their critical and helpful comments. We have responded to all of them below and tried to address as many as possible to significantly improve the manuscript. For the few cases where we did not follow the reviewers' suggestions, we discuss the reasons for our decision. The referee comments are displayed in italics, followed by our responses in normal font.

5 **Anonymous referee #1**

Schaller et al. use a new technique for measuring snow that aims for pristine sampling of the top 2 meters for retrieval and analysis in the laboratory, and present a dynamic time warping (DTW) feature alignment method. The authors construct an average density profile for the North Greenland ice sheet and compare accumulation rates, melt layers and isotopic values in the area over several years. The sampling technique and CT system are very nice, the analysis is sophisticated and thoughtful.

10 *What isn't clear is how representative the product is, the density profile.*

The authors include significance testing of their density alignment, which is a good idea. However, the actual numbers are marginal. The analysis uses artificial data to compare correlation coefficients for real versus fake data sets, but the resulting coefficients are not that much higher for real data.

Indeed, the numbers are not that much higher. However the main cause for this fact is that we compare with the most realistic
15 surrogates that we were able to create. The artificial datasets consist of the real $\delta^{18}\text{O}$ profiles and a density signal based on the seasonal cycle, a $\delta^{18}\text{O}$ -density relation and a statistical model with three components for the stratigraphy. If we use a simple statistical method (e.g. autoregressive processes) we can generate much more impressive numbers, but instead we wanted to show that even in comparison to surrogates with the maximum amount of real information there is a small, but significant difference. We tried to clarify this in the manuscript by adding more details in Chapters 3.2 and 5.1.

Why are the density profiles smoothed before covariance testing? Are the fake data sets also smoothed in evaluating significance?

As can be seen in Chapter 4.1, last paragraph, we mainly work at the base resolution of 0.1 cm for covariance testing, which corresponds to no smoothing. We only wanted to provide the information that the shared variance increases with smoothing, which can be explained by the steady transformation into a seasonal signal. Apart from that statement, all of the numbers in this paragraph refer to the base resolution and are indicated to do so.

Comparing example profiles in Figure 6, and the example representative profile in Figure 7 with its substantial one-sigma confidence interval, it's hard for the reader to judge what is being captured or how useful it is. The bottom two-thirds of the representative profile in Figure 7 is consistent with a straight line.

In order to improve the understanding of the presented content, the following has been added to the discussion of Figure 7 in Chapter 5.1: "For the given error band, there is an overlap of uncertainty in the depth alignment (x -direction) with the uncertainty in density (y -direction). The former is mainly caused by the variability of the snow mass accumulated from a single deposition event. Regarding the latter, the average density of the snowpack greatly varies as can be seen in Fig. 9. Thus, for the second meter, even though it is contained in the uncertainty band, we do not expect a straight line, but rather an alternation of high and low density layers similar to the upper meter."

This is not the first time that DTW or other speech/biometric processing approaches have been adapted for stratigraphic alignment of environmental records, or even ice core records, and Schaller et al. may benefit by referring to these and other probabilistic approaches.

Three additional references have been added to Chapter 3.1 to provide an adequate overview of previous research - a detailed review of the DTW method (Senin, 2008), an example of its application in polar science (remote sensing of ice floes, McConnell et al., 1991) and a recent example for a different approach to align physical properties within the snowpack (Hagenmuller and Pilloix, 2016).

DTW is most effective when aligning time series containing prominent features that are highly similar. Since the goal (based on the manuscript title) is an average profile, it would be useful to check consistency between the various record alignment combinations, e.g., the features matched between N2E_04 and N2E_05 with NEEM, should also match between N2E_04 and N2E_05 with each other.

We apologize, this has actually been checked but not stated. "There were no notable differences when another location (e.g. EGRIP) was chosen as the reference or the fitting was done consecutively." was added to Chapter 4.1.

Technical corrections, typos and style:

Abstract, line 5: suggest striking "based"

Done.

Section 2.2, line 29: "...a worldwide unique..." suggest striking "worldwide"

Done.

Section 3.1, line 22: "...could be fit to arbitrary many..."

Changed to "a single value of one data set could be fit to arbitrarily many of the other."

5 Section 4.1, line 11.

Removed extra "of", replaced "fit" by "fitted" and "liners" by "profiles".

Anonymous referee #2

General comments: This paper presents a new technique for efficiently retrieving shallow snow and firn cores from polar regions. Those cores can then be returned to a lab for high-resolution analysis using a micro-CT scanner. These types of
10 *measurements are needed to better understand the evolution of firn, which in turn will lead to more accurate estimations of mass-balance changes on the ice sheets. The authors apply a technique that was developed for speech recognition, Dynamic Time Warping (DTW), to analyze changes in snow and firn properties along a 450-km traverse in northern Greenland. Additionally, the authors examine variability in annual accumulation rates and relationships between water isotopes (a temperature proxy) and accumulation rates. The paper makes a valuable contribution to the glaciological community and will be of partic-*
15 *ular interest to those who study snow and firn related surface-mass-balance processes and ice-core delta age estimation. The “liner” technique combined with DTW could easily be adopted by the snow-hydrology and snow-avalanche communities to investigate snow properties on smaller spatial scales. I have 2 general comments and numerous specific comments that I would like to have addressed before publication.*

“Matching” snow and firn properties. The authors use DTW to “match” the firn properties along the traverse. The first step
20 *of the alignment is to match the $d18O$ data, which identifies snow/firn from a particular summer or winter. This seems to me to be the most valuable use of the DTW technique because it gives an idea of how accumulation is varying seasonally and annually over a large distance (temporal and seasonal variability). Their next step is to align high-resolution density features in the snow/firn. However, I am left unsure what information this high-resolution matching or alignment is providing. What is the end goal in aligning the high-resolution density data? Is it to track layers deposited during individual weather events? Or*
25 *to provide a common depth-age profile along the traverse?*

The goal is to track features (melt layers, wind crusts as well as significant changes in density at the borders of snow layers from different "events") to learn about their spatial extent and variability. Then, the fact that we are able to do so, enables us to provide a common depth-age profile and construct a representative density profile for the traverse region (cf. Chapter 3.1). The profile can be rescaled to any location of known accumulation. Amongst others, it may be applied as a benchmark for

snowpack models or for the detection of strong density gradients as potential reflectors in remote sensing (for further details, see Chapter 6).

Related to this question: What does the "fine fit" in Figure 4b mean physically, and why is that a useful metric?

The mass accumulated by a certain event is strongly influenced by wind speed and direction (Fisher et al., 1985, cited), which are partially coherent over the region of interest (Chen et al., 1997, cited). Due to diffusion, this information might be lost post-depositionally in the $\delta^{18}\text{O}$ signal, which also has a pretty low resolution compared to the vertical extent of features (e.g. melt layers) in the snow (cf. Chapter 3.1). Thus fitting the seasonal $\delta^{18}\text{O}$ signal provides a coarse "age"-alignment of the snow, but no "feature"-alignment. Densities, on the other hand, are available at a much higher resolution and less likely to be influenced post-depositionally. This makes the second ("fine") fitting step (see also, Results, 4.1, reference to Figure 4) necessary and useful.

Likewise, what is the physical meaning of the color bands in Figure 6? Would those be layers of snow with the same age?

The color bands do not represent physical layers, but snow of potentially the same origin and thereby approximately the same age. This is described in the figure caption: "... A colormap was applied uniformly at the first position (NEEM) and then transformed the same way as the depths were aligned. Thus snow within the same color band was matched during the fitting process..."

I believe that using DTW on the high-resolution density data includes an a priori implicit assumption that stratigraphic features (layers) are continuous (or at least correlated) over hundreds of kilometers, but the authors have not convinced me that this is or should be true. Why do you expect the depth-density profiles to be related? Does this argument hold up if this assumption is not true? Recent work by Proksch and others (2015, e.g. Fig. 12) showed significant stratigraphic variability in the near-surface snow in Antarctica. I would expect some amount of coherence on the 10's-of-kilometers scale, but it is surprising to hear that stratigraphic features (and coherence in density) persist over hundreds of kilometers and over a divide, where temperatures and accumulation rates vary on daily to annual time scales. If the authors are assuming that layers persist over these distances, at what layer resolution would they expect this assumption to break down? Can you be confident that the algorithm is matching real layer correlations and not just recognizing stochastic layering that all happens to fall near some mean density? The authors do discuss verification of their method using surrogate density profiles. However, I do not follow their reasoning – this could be a place to clarify their language.

Our plan was to identify features in consecutive profiles and steadily expand a continuous depth alignment (as in Figure 6). Thus, the a priori assumption of our work was being able to track stratigraphic features over 20-30 km in agreement with your expectations. It was not our initial intention to trace layers over hundreds of kilometers. We started by fitting the profiles consecutively, which does not significantly change the results. A sentence with this statement has been added to Chapter 4.1. Potential reasoning for coherence in the density profiles over larger distances is given (e.g. predominant origin of weather and precipitation - see Chapter 6, Line 13-16). Regarding the ice divide, it is visible in the RMSE as discussed (cf. Figure 5; Chapter 5.1, L 4-7). As we mentioned above, we do not aim to identify "layers" in a physical sense, but significant changes in snow

properties. Therefore there is no "resolution" where the fitting would break down, apart from when features become smaller than the base resolution of our density alignment (i.e. 0.1 cm). We further used surrogate density profiles to test whether the increased shared variance after the fine tuning step could be explained by chance. The results show that the amount of shared variance for the measured profiles is statistically significant, which underlines that we are not just recognizing stochastic layering.

The mentioned paper shows data from Kohnen Station, which is located in an East Antarctic low-accumulation region (64 mmWE/a) and thus comparison with our traverse (115-225 mmWE/a) is not straightforward. Indeed, there is significant wind scouring (possibly causing hiatuses of the complete mass accumulated by a single event) at Kohnen (compare e.g. Muench, 2015, cited).

10 *Ultimately, the authors do not make a strong case to me that the layers they are fitting are spatially extensive and not stochastic noise. I request that the authors justify the assumption that the layers are spatially extensive. Additionally, they should clarify the language of what the alignment using high-resolution depth-density data means. An example of somewhere to clarify: Page 5 Line 4 says, " ... the continuous depth scale agrees ... " Perhaps specifying what a continuous depth scale means would help me understand – is that a continuous depth-age scale? Alternatively, the authors could focus on the DTW using the $\delta^{18}\text{O}$ data.*

15 The statistical verification shows that there is a significantly increased shared variability between the real density profiles compared to surrogate data (which we tried to design as realistic as possible, e.g. the original $\delta^{18}\text{O}$ profiles were used). Thus we provided evidence for spatial coherency of the density over hundreds of kilometers. Further details have been added to Chapters 3.2 and 5.1 to clarify this, see also first answer to RC #1. We tried to put more emphasis on showing the value of having the densities for high-resolution alignment and apologize for the misleading term "continuous/moving depth scale", that was replaced by "depth alignment" (e.g. the color bands in Figure 6). Apart from statistical analyses (as already carried out), proving the existence of spatially extensive layers would require an extremely dense sampling of the stratigraphy, which is not achievable. Indirect methods, such as high-resolution shallow radar (e.g. Hawley et al., 2006, cited), indicate the persistence of layers over 10's to 100's of kilometers, but do not provide the vertical resolution to validate layer structure on the same scale as our approach.

25 *Uncertainty and application to mass balance. The authors point out in the introduction the importance of knowing firn properties for mass balance calculations, and they derive a representative depth-density profile. How much uncertainty is associated with using this representative profile? I suggest that it would be useful to compare the representative depth-density profile to measurements and model predictions. A metric of interest for the mass-balance community is the depth-integrated porosity (DIP), or the amount of air in the snow and firn. I think it would be a useful exercise to compare the DIP that is observed in the cores to the DIP that is predicted by the representative profile. Additionally, it could be compared to the DIP predicted by assuming some constant density for the top 2 m and perhaps to density profile predicted by a firn-densification model.*

An error band for the representative profile is given in Figure 7, further explanation regarding uncertainties has been added to Chapter 5.1. We have discussed this point and unfortunately do not see a considerable merit in calculating the DIP for two

meters of snow, where we only expect marginal differences. To our knowledge it is a parameter that is rather interesting with respect to the whole firn column. In addition, the DIP for a density profile will only be determined by its average value – the formula is $DIP = 2m \cdot (1 - \frac{\rho_{avg}}{\rho_{ice}})$. Instead, we see the main advantage of a high-resolution density profile for remote sensing in the opportunity to determine significant density contrasts that can cause strong reflections (such as the 2012 melt layers).

- 5 To clarify this in the manuscript, we also changed the respective sentence in Chapter 6 to "Thus it [the representative profile] is ready to act as a benchmark for snowpack models or be applied for the conversion of volume to mass and the detection of strong density gradients as potential reflectors in remote sensing." Furthermore, there is no significant firn-densification in the upper two meters (compare sample density curves, e.g. Figure 6).

Specific comments: - Page 2, Line 4: thereby measurements of what?

- 10 Corrected.

- P2, L10: what individual parameters?

Density, $\delta^{18}\text{O}$ and accumulation rate. Added.

- P2, L20: How do you know in which cases the snow might be compacted?

- 15 The tube has no lid or similar. Thus, as you push it into the snow, at some point the top of the liner will be parallel to the surrounding snow surface. If the snow inside the liner is not, it has been compacted.

- P2, L28: Are you confident that no metamorphism occurs during transport, e.g. due to temperature gradients?

- 20 We transport the samples with the minimal number of transitions at a constant (low) temperature, the same way it is done for ice cores (e.g. NEEM). This minimizes the effects of isotopic diffusion and potential metamorphism (e.g. there is no long exposition to temperature gradients). Currently we do not know about any significant impact of such transport on the conducted measurements (2D density profiles, $\delta^{18}\text{O}$). For example, a comparison of discrete density measurements on a trench wall close to Kohlen station and CT density measurements of liners transported to Bremerhaven showed good agreement.

- P2, L31: "Amongst others, ..." amongst other what? Other corrections? If so, state what those are.

A more detailed description of the AWI-Ice-CT and its measurement procedure has been provided in previous publications (e.g. Freitag et al., 2013, cited). This has been clarified in the manuscript.

- 25 *- P3, L24: a shift in what?*

"in depth" added.

- P3, L26: what do you mean by event?

"deposition" added.

- P3, L26: what do you mean by align? (related to general comment above) Snow of a certain age?

"of the same origin" added.

- P3, L30 – P4: DTW is a complicated concept to read through for the first time – perhaps you can provide an example in this section – e.g. what “assigning the values of” means, what “proceeding through the matrix” means, etc.

We added an introductory reference to the manuscript as DTW is already a well-described method.

5 - P5, L3: Combine all of the available information: are you using anything besides d18O and density?

No. Removed "all".

- P5, L9/Table 2: How did you come up with you maximal/minimal offset values? (Should that be maximum/minimum?)

Maximum, yes. We added the sentence "The maximum allowed offsets for the coarse fitting have been chosen according to the measured height of variations in the snow surface (e.g. dunes) and the maximum ratio of estimated accumulation rates. In
10 the second step we allow for fine tuning up to the maximum remaining shift, that was manually identified by aligning the 2012 melt layers." to Chapter 3.1.

- P5, L12: These aren't really continuous, are they? You have discrete measurements from every 25 km along the traverse. How do you interpolate between those?

The term "continous" refers to being able to connect the profiles here. We do not use interpolation as part of our analysis, but
15 if we interpolate for visual purposes (e.g. Figure 6) it is done linearly. This has been indicated in the manuscript.

- Section 3.2: Are the statistics informing the creation of the surrogate density profiles taken from the bulk of all geographic locations (i.e. sigma_base is the standard deviation from all sites) or from single sites?

From single sites. "independently" added to the first paragraph of 3.2 to clarify.

- P5, L24: Do you calculate the surrogate profiles for each site individually using that site's statistical properties, or the bulk
20 statistical properties of all sites?

Added another "For each site" in the third paragraph.

- P6, L12: How do you define a “layer”?

Replaced by "snow of similar properties".

- P7, L9: How is 0.1m chosen as the maximum allowed shift?

25 See previous question/answer regarding maximum allowed shifts (P5, L9/Table 2).

- P7, L10: What does “all combinations of 2 liners” mean? Do you mean that you are comparing the 2 meters of data from each site to each other site?

Yes. Replaced by "all combinations of profiles from two sites".

- P7, L11-12 and P9, L1: *Can you further elaborate on why that change occurs? Going over the divide, you lose some coherence, but not all? Which signals are lost going over the divide, and which are maintained? Is there also a change at the 1/2 way mark?*

Yes, we lose some coherence in the divide area, but not all. To us, it is not straightforward to talk about lost or maintained "signals" here as there is no separate "signals" identified in the matching process but whole profiles compared. The idea of Figure 5 was to provide an overview, which visualizes a change in snow structure or stratigraphy at a position that coincides with the area where the divide was left. There could be a change at the 1/2 way mark in Figure 5, but the differences between N2E_11 and the neighboring sites might be misleading. However, it is less prominent than the one at the ice divide. In order to be more precise, the caption now reads "The most notable change in snow structure can be observed between the fourth and the fifth column (or row)."

- P7, L15: *It is unclear to me: was the representative density profile created by stacking the raw depth-density data, or by using the "aligned" profile from DTW?*

The respective sentence now reads "Using the previously calculated depth alignment, density records were stacked to obtain a representative density profile", which should clarify the aligned profiles were stacked.

15 - P8, L9: *Do the high and low accumulation years correlate spatially? I.e. does a high-accumulation year at NEEM also mean high accumulation at EGRIP?*

Previous sentence: "Comparing average values for the different years there is neither a trend nor considerable variations in the accumulation rate (cf. Table 4)." There is no spatial correlation of low and high accumulations, as this would cause considerable variations of the annual averages.

20 - P8, L12: *Is this spread in isotopic coldest year surprising? Are those data corroborated by reanalysis (e.g. RACMO) data?*

We feel that including reanalysis data to discuss this point would be beyond the scope of our manuscript. This information is solely provided for the interested reader.

- P8, L18 and Figure 10: *What is the source of those outliers? Sampling/instrument error? Please elaborate on how you identified them as such.*

25 We apologize, the term "outlier" was incorrectly used here and has been replaced/avoided. The large spread in 2013 cannot be explained by sampling or instrumental errors.

- P8, L20-21 (and P10,L16): *I think it would be appropriate to elaborate on why the summer snow has a lower density.*

Added "The main causes given are the increased packing due to stronger winds in winter and the larger size of precipitation particles in summer." in 5.3.

30 - P9, L12: *Why do you not expect significant compaction? Reference or justify.*

"Densification" would have been the more precise term here. We would be able to observe it in the density profiles (increasing average value). Sentence changed to "Furthermore we do not observe significant densification ..."

- P10, L6: *Why is the winter picture less clear?*

Chapter 4.2, last paragraph. Different years have been coldest for different sites. "Furthermore" replaced by "Indeed" to better link to the following sentence (surface signal might still change).

- P10, L9: *You show that warmer sites have more accumulation. For a given site, does a warmer winter, summer, or year correlate with higher accumulation at that site?*

We do not observe such correlation, the amount of snow accumulated in a certain year seems to mainly be determined by the surface variations.

10 - *Figure 3: Does not clarify the constraints on stepping to me.*

"Here usage of cell $[i, j]$ refers to $\mathbf{S}[i]$ being assigned to $\mathbf{T}[j]$." added to 3.1, after reference to Figure 3.

- *Figure 6: The densities that are plotted do not have labels, scales, or units. Are those the centerline values and scales same for each? It might be helpful to mark the mean density and standard deviation of each of depth-density profile.*

Caption of Figure 6 changed to "In black, measured density profiles for the labeled positions are shown at the same scale, centered around their respective mean values." We have tried adding more information regarding the example density profiles to the plot but fear that it will decrease the clarity and thus make it more difficult for the reader to grasp the essential information. In addition, there are other plots (e.g. Figure 4) showing densities with scale and unit.

- *Figure 7: What are your x and y directions? Can you elaborate on how you get the standard deviation error band, e.g. is it comparing the raw data from each site to the representative profile?*

20 The following has been added to the discussion of Figure 7 in Chapter 5.1: "For the given error band, there is an overlap of uncertainty in the depth alignment (x -direction) with the uncertainty in density (y -direction). The former is mainly caused by the variability of the snow mass accumulated from a single deposition event. Regarding the latter, the average density of the snowpack greatly varies as can be seen in Fig. 9. Thus, for the second meter, even though it is contained in the uncertainty band, we do not expect a straight line, but rather an alternation of high and low density layers similar to the upper meter."

25 *Technical corrections: - Numerous places in text the authors use vague language: e.g. "profile" (depth-density profile, depth-age, density-age profile, "depth profile" is still vague), "position" (position could refer to some point on the firn core rather than a geographic location, and I suggest a change to "site" or similar)*

"Position" replaced by "site" or "location". Regarding "profile": The term "depth profile" is not used in the manuscript. We did use the terms "density profile", " $\delta^{18}\text{O}$ profile" and "isotope profile", which implies depth is the second parameter when talking about snow or ice cores. The term "profile" is solely used when the respective property is clear from the context or no specific property is addressed. We hope that this satisfies the reviewer's comment.

- Throughout: The authors use the language “the liners show” or similar (e.g. P5L12); the “liners” are the instruments/tools used to gather their data and are not what actually show anything. I suggest language such as “the data from each of the sites show”

The mentioned sentence now reads "For all sites we find at least two melt layers in the snow isotopically dating back to the summer of 2012." Similar language has been changed throughout the manuscript.

- There are numerous instances throughout the manuscript where (1) commas are misused or lacking and (2) hyphens are needed.

We reread the manuscript carefully and tried to follow the TC guidelines as closely as possible. Please note that these partly differ from the guidelines of other publishers or standard dictionaries.

10 - Several places in the text change tense (past vs. present, e.g. section 2.1) and voice (active vs. passive). I suggest choosing one.

2.1. was written in present tense on purpose, in order to describe a new technique. It has been updated to past for consistency now.

- Page 1, Line 5: *empirical based empirically-based*

15 "based" was removed.

- Page 1, Line 11: *impact impacts*

Both seems possible. We do not see why "impacts" would be better here.

- Page 2, L1: *causing creating*

Both possible, wanting to be precise the warm days did not really "create" the melt layers though.

20 - P2, L25-26: *probing sampling, “that technique” “the liner technique”*

"Probing" replaced by "sampling", "that technique" removed.

- P3, L3: *measurement time increases with resolution? (rather than accuracy)*

Changed, we tried to avoid too many repetitions of "resolution" and replaced the next instance by "pixel size" instead.

- P3, L5-6: *“Then, the raw ... CT images.” Unclear sentence*

25 Extra "the" removed.

- P3, L7: *weight mass*

Replaced.

- P3, L15-16: clarify that is it 3-5 years worth of accumulation contained in the 2-m sample; specify “winter-to-winter accumulation rates”

Both done, the paragraph now reads "Using the density data, accumulation rates at the different sites were calculated from the snow mass for the three to five years worth of accumulation contained in the top two meters of the snowpack. In the present study, we only use winter-to-winter rates (separating years at the $\delta^{18}\text{O}$ minima) – summer-to-summer values were computed as a reference but show no different behaviour."

- P3, L21: renowned well-known

Done.

- P4, L23: what does the “maximal ratio of the respective accumulation rates” mean? Respective to what? Two sites next to one another?

Yes. Clarified by adding "between two sites".

- P6, L3: Perhaps use z_i since you are talking about depth. The x dimension (to me) indicates a direction on the surface (e.g. along your traverse).

Changed.

- P7, L15: Change to “The previously-calculated depth-scale density records were stacked to obtain...”

Changed.

- P8, L6: Increasing to 140 where?

"at EGRIP" added for clarity.

- P9, L1: fourth liner? Do you mean location/site?

Yes, "liner" replaced by "site".

- P9, L15: The statistics in this paragraph were already reported on page 7; did you intentionally do that?

Yes. In order to improve the manuscript, one more repetition was omitted. All remaining numbers are directly referred to.

- P9, L21: is are, summer of 2012

Corrected.

- P9, L27: sommer summer

Corrected.

- P10, L20: accustic acoustic

Corrected.

- *Figure 8: y-axis does not have scale or units labeled*

On purpose. "Each profile is displayed at the same scale and has been centered around its mean." added to caption.

- *there are numerous instances of typos and challenging-to-read sentence structure that I have not indicated here; I recommend*
5 *having a copy editor review the manuscript for those.*

Reference: Proksch, M., Löwe, H. & Schneebeli, M. (2015). Density, specific surface area, and correlation length of snow measured by high-resolution penetrometry. Journal of Geophysical Research: Earth Surface, 120(2), 346-362.

Marked-up manuscript – "A representative density profile for the North Greenland snowpack"

Christoph Florian Schaller¹, Johannes Freitag¹, Sepp Kipfstuhl¹, Thomas Laepple², Hans Christian Steen-Larsen³, and Olaf Eisen^{1,4}

¹Alfred Wegener Institute, Helmholtz Center for Polar and Marine Research, Bremerhaven, Germany

²Alfred Wegener Institute, Helmholtz Center for Polar and Marine Research, Potsdam, Germany

³Centre for Ice and Climate, Niels Bohr Institute, University of Copenhagen, Denmark

⁴Department of Geosciences, University of Bremen, Germany

Correspondence to: Christoph Schaller (christoph.schaller@awi.de)

Abstract. Along a traverse through North Greenland in May 2015 we ~~sampled the top two meters of snow and analyzed its~~ collected snow cores up to two meters depth and analyzed their density and water isotopic composition. A new ~~technique for~~ probing the upper meters of the snow sampling technique and an adapted algorithm for comparing data sets from different ~~positions sites~~ and aligning stratigraphic features is presented. We find good agreement of the density layering in the snowpack
5 over hundreds of kilometers, which allows the construction of a representative density profile. The results are supported by an empirical ~~based~~-statistical density model, that is used to generate sets of random profiles and validate the applied methods. Furthermore we are able to calculate annual accumulation rates, align melt layers and observe isotopic temperatures in the area back to 2010. Distinct relations of $\delta^{18}\text{O}$ with both accumulation rate and density are deduced. Inter alia the depths of the 2012 melt layers and ~~high-resolution~~ high-resolution densities are provided for applications in remote sensing.

10 1 Introduction

In the context of global warming, the Greenland ice sheet has been identified as a so called "tipping point" of climate change (Lenton et al., 2008). The sea level rise caused by its decay may have severe impact on human society as well as ecological systems. Thus the difference in accumulation across the interior of the ice sheet and seasonal melting, runoff and calving at its borders, the so called mass balance, has been in the focus of recent scientific activities in the Arctic region. The applied
15 methods for its determination range from satellite remote sensing (e.g. Zwally et al., 2011) ~~over~~ regional climate modeling (e.g. Fettweis, 2007) to large scale climate simulations constrained by weather station data and ice core records (e.g. Hanna et al., 2011). Even though first accumulation and density measurements were already carried out in 1952 – 54 (Bull, 1958) using accumulation stakes and Rammsonde measurements at a few points alongside the gravity survey of the British North Greenland Expedition, large scale studies such as Benson (1962) are still very rare. To obtain accumulation maps of Greenland
20 such as Bales et al. (2009) diverse data sets from ice cores, snow pits and weather stations have to be collected over several years. Recently Hawley et al. (2014) conducted a ground-penetrating radar survey alongside a traverse of about 1000 km length,

supported by a few snow pits and shallow cores for bulk densities and chemical profiling. Koenig et al. (2015) used airborne snow radar to determine accumulation rates from 2009 to 2012 along flight paths of more than ten thousand kilometers.

In summer 2012, there were two very warm days with temperatures above 0°C almost all over Greenland, causing substantial melt layers (Nghiem et al., 2012). Although this was a very rare event induced by a special weather situation (Bennartz et al., 2013), the newly formed ice layers strongly influence the physical properties of ~~the snow and firn pack and thereby also measurements~~ (Nilsson et al., 2015).

We introduce a new and efficient technique for sampling the snowpack along traverses, which allows for additional lab-based measurements to gain ~~high-resolution~~ high-resolution profiles of physical snow properties, such as density. Furthermore we adapt an algorithm from speech recognition to align those spatially distributed data sets and provide further insight into their development with changing surrounding conditions. The method is tested with randomly generated sets of density profiles with the same statistical properties as the original measurements. As an application we present data gained along a 450 km traverse in North Greenland, deduce relations of the individual parameters ~~and (density, $\delta^{18}\text{O}$ and accumulation rate) and~~ show additional values of interest such as the depths of the 2012 melt layers.

2 Data acquisition and processing

In preparation for the upcoming East Greenland Ice core Project (EGRIP), the Danish Center for Ice and Climate's dome and equipment had to be moved about 450 km from the previous drilling site, NEEM. Alongside this so called "N2E" traverse in May 2015 several measurements of the upper part of the firn and the snow surface were undertaken. Amongst others, the upper two meters of the snowpack were sampled using the "liner technique" described in detail below. Snow cores were taken approximately every 25 km at the ~~positions~~ sites shown in Fig. 1, detailed coordinates can be found in Table 1.

2.1 Liner technique

The sampling ~~is was~~ done using carbon fibre tubes with sharp edges of one meter length, ten centimeters diameter and one millimeter wall thickness (called "liners"). To start off, the first liner ~~is was~~ carefully pushed and hammered into the ground until its top ~~is was~~ parallel to the snow surface. Nonetheless in a few cases the snow ~~inside the tube might be core was~~ slightly compacted by up to two centimeters in the vertical direction, visible as a reduction of the snow level inside the tube compared to the surroundings. Subsequently a snow pit of one meter depth ~~is was~~ dug next to the tube and the snow cut off at its bottom using a metal plate or small saw. The tube ~~is was~~ removed and its openings sealed using matching plastic bags. Then the cutting surface ~~is was~~ cleaned and the second liner inserted right below the first one. Finally the pit ~~has had~~ to be deepened to two meters to once again cut off the snow and take the second liner. Theoretically the described process can be iterated up to an arbitrary depth. However, the area of the required snow pit increases significantly with every meter of depth gained. ~~Probing~~ Sampling the upper two meters ~~by that technique takes took~~ approximately two hours per site.

2.2 X-ray tomography

The cores were transported to the ~~Alfred Wegener Institute~~Alfred Wegener Institute, Bremerhaven, in frozen condition. All samples were analyzed in the AWI-Ice-CT (~~Freitag et al., 2013~~), ~~a worldwide~~(described in detail in Freitag et al., 2013), a unique X-ray computer tomograph in a cold lab, which allows μm ~~resolution~~resolution density measurements of whole one meter core segments in 2D and 3D. As part of the measurement procedure a sample holder for liners was constructed, that itself contains several pieces of pure ice of known geometry for calibration purposes. Amongst others, the effect of the carbon fibre tube being part of the scan was corrected for ~~r~~using empty tube measurements. Thus, the fragile snow cores do not have to be removed from the liners.

As the required measurement time increases with ~~accuracy~~resolution, we chose to do 2D scans with a ~~resolution~~pixel size of approximately 0.128 mm. Each of these scans takes about three minutes. However, fifteen minutes per meter are more realistic when including sample preparation and accurate documentation. Then, the raw measurement data are automatically processed by detecting the calibration unit and directly calculating densities from the ~~the~~ CT images. Additionally, for each liner, the mean density is determined from the ~~weight~~mass and geometry of the snow as an independent comparison value. Figure 2 displays an example CT image with a zoomed section showing two melt layers in the snowpack aligned with the respective densities derived from 2D analysis.

2.3 Isotope measurements

Finally, the snow was gently pushed out of the tubes and cut in samples with a vertical height of one centimeter for the 30 cm right below the surface and two centimeters otherwise. These samples were crushed and sealed in plastic bags. Finally water isotopes were measured using a Picarro L2130-i with a precision of $\sigma = 0.1\%$ for $\delta^{18}\text{O}$.

The snow was dated by determining and counting the maxima (summer) and minima (winter) in the seasonal $\delta^{18}\text{O}$ signal. Using the density data, accumulation rates at the different sites were calculated from the ~~ice mass at the different sites for the contained snow mass for the~~ three to five years worth of accumulation contained in the top two meters of the snowpack. In the present study, we only use ~~winter-to-winter rates~~winter-to-winter rates (separating years at the $\delta^{18}\text{O}$ minima) – ~~summer-to-summer~~summer-to-summer values were computed as a reference but show no different ~~behaviour~~behavior.

25 3 Mathematical methods

3.1 Automatic alignment of stratigraphic features

In order to efficiently analyze the data sets generated along the traverse, we investigated several ways to automatically detect coherent signals at the different ~~positions~~sites. ~~A renowned~~A well-known matching method is maximizing the ~~cross correlation~~cross-correlation. However, determining a constant shift in depth between two profiles is not suitable for our case as the accumulation rate, and thus the vertical spacing of layers, is subject to change going eastwards. Under the assumption of constant accumulation over time and no significant compaction in the top two meters, one would expect a shift which is linearly

increasing with depth and has a slope equal to the ratio of accumulation rates. Then again, local environmental conditions such as wind speed and direction influence the mass accumulated by a certain deposition event (Fisher et al., 1985). Therefore we aimed to align snow of the same origin and its properties with continuously changing shifts, a problem that has already been worked on at a lower vertical resolution for alpine snow (e.g. Hagenmuller and Pilloix, 2016).

5 The Dynamic Time Warping (DTW) method, that was introduced to speech recognition in the seventies (Itakura, 1975), provides an efficient algorithm for that purpose. It has already been applied in numerous fields, e.g. for the tracking of ice floes in SAR images (McConnell et al., 1991). For a detailed review of DTW, see Senin (2008).

The basic idea is to discretize the two data sets to be compared with the same step size l (resulting in two vectors \mathbf{S} and \mathbf{T} of length n and m) and then consecutively assign the values of one to another, whereby each value can be matched with multiple
10 values of the other data set. To find the best fit, one calculates a matrix $\underline{\mathbf{D}}$ where $\underline{\mathbf{D}}[i, j]$ indicates the error of the best path that leads to the i 'th element of the first data set being connected to the j 'th element of the second one.

The original algorithm starts by calculating the matrix in the upper left corner, fixing the first elements of both data sets to be linked with each other. Then it proceeds through the matrix by taking the path with the minimal error leading to the respective cell and adding the local error, i.e.

$$15 \quad \underline{\mathbf{D}}[i, j] = \begin{cases} \infty & \text{for } i < 0 \text{ or } j < 0 \\ \|\mathbf{S}[0] - \mathbf{T}[0]\| & \text{for } i = 0 \text{ and } j = 0 \\ \|\mathbf{S}[i] - \mathbf{T}[j]\| + \min(\underline{\mathbf{D}}[i, j-1], \underline{\mathbf{D}}[i-1, j-1], \underline{\mathbf{D}}[i-1, j]) & \text{else.} \end{cases} \quad (1)$$

Finally, ~~it goes to on arrival at~~ cell $\underline{\mathbf{D}}[n, m]$ ~~and it~~ backtraces the path of minimal errors to $\underline{\mathbf{D}}[0, 0]$, obtaining the best fit of the complete data sets in the given norm $\|\cdot\|$.

For our application – matching measurements of the upper two meters of the snowpack – we do not aim to fit complete data sets, but rather allow for different offsets at the top and bottom. The former may be caused by variations of the snow surface
20 due to current conditions, the latter by different accumulation rates leading to data at the bottom of the liners not having any physical relation apart from being the deepest snow analyzed at the given positionlocation. To accomplish that, we expand the idea of Sakurai et al. (2007) introducing maximal surface and bottom index offsets s and b . Then we initialize $\underline{\mathbf{D}}$ by

$$\underline{\mathbf{D}}[0, j] = \|\mathbf{S}[0] - \mathbf{T}[j]\| \text{ for } 0 \leq j \leq s \text{ and} \quad (2)$$

$$\underline{\mathbf{D}}[i, 0] = \|\mathbf{S}[i] - \mathbf{T}[0]\| \text{ for } 0 < i \leq s \quad (3)$$

25 before proceeding through the matrix. Finally instead of backtracing simply from $\underline{\mathbf{D}}[n, m]$, we end our fitting path at

$$\min \{ \underline{\mathbf{D}}[i, j] \mid (i = n \text{ and } m - b \leq j \leq m) \text{ or } (j = m \text{ and } n - b \leq i \leq n) \} \quad (4)$$

and search a trace back to any of the initialized elements. Thereby we find the best matching of subsets of S and T with a maximal shift of $s \cdot l$ at the top and $b \cdot l$ at the bottom. In between, we verify that a linearly increasing maximal shift is not exceeded.

The simple way we proceed through the matrix so far, often referred to as "stepping pattern", is unrealistic for our case as a single value of one data set could be fit to ~~arbitrary-many-values~~ arbitrarily many of the other ~~data-set~~. Along the traverse we find the maximal ratio of the respective accumulation rates between two sites to be a little smaller than two. Therefore, we apply a constrained stepping as presented by Sakoe and Chiba (1978) such that each value of one data set can be fit to at most two values of the other. This is obtained by

$$\underline{\mathbf{D}}[i,j] = \begin{cases} \|\mathbf{S}[i] - \mathbf{T}[j]\| + \min(\underline{\mathbf{D}}[i,j-1], \underline{\mathbf{D}}[i-1,j-1], \underline{\mathbf{D}}[i-1,j]) & \text{for } i = 1 \text{ or } j = 1 \\ \|\mathbf{S}[i] - \mathbf{T}[j]\| + \min \begin{pmatrix} \|\mathbf{S}[i-1] - \mathbf{T}[j]\| + \underline{\mathbf{D}}[i-2,j-1] \\ \underline{\mathbf{D}}[i-1,j-1] \\ \|\mathbf{S}[i] - \mathbf{T}[j-1]\| + \underline{\mathbf{D}}[i-1,j-2] \end{pmatrix} & \text{else.} \end{cases} \quad (5)$$

Figure 3 illustrates the different patterns for proceeding through the matrix. Here, usage of cell $[i,j]$ refers to $\mathbf{S}[i]$ being assigned to $\mathbf{T}[j]$. In the aftermath, the backtracing has to occur according to the implemented stepping.

Finally, we do not only want to fit one type of data (e.g. densities) but combine ~~all~~ the available information in the profiles to gain a robust picture of the developing stratigraphy along the traverse. In a first step, we match the $\delta^{18}\text{O}$ signal, which shows a clear seasonal behavior but almost no ~~small-scale~~ small-scale variations as the ~~high-frequency~~ high-frequency component is lost by diffusion. Then, we use the obtained depth assignment of the two different ~~positions~~ sites to resample the measured densities to a common depth scale. In a second step, we apply the algorithm to these densities at a much higher resolution to ~~fine-tune~~ fine-tune our depth alignment according to ~~small-scale~~ small-scale stratigraphic features. As a norm we use the Euclidean distance divided by the path length (i.e the root mean square error), which means that we have to keep track of the path lengths in a second matrix. Table 2 summarizes the final set of parameters. The maximum allowed offsets for the coarse fitting have been chosen according to the measured height of variations in the snow surface (e.g. dunes) and the maximum ratio of estimated accumulation rates. In the second step we allow for fine-tuning up to the maximum remaining shift, that was manually identified by aligning the vertical centers of the 2012 melt layers.

This method does not only allow us to compare data from two ~~positions~~ sites, but also to obtain a moving depth ~~scale~~ alignment by fitting the ~~liners~~ profiles to the first data set one by one. The result, a continuous image of the snow layering, can be compared with other indicators such as the melt layer positions. In addition, being able to align densities and stratigraphic features all along the traverse enables us to provide a representative density profile for the region. For its construction, we first use the continuous layering to transform all density curves to the first depth scale (NEEM) and average them. This, however, is not yet a representative density profile as all profiles now replicate the layering at NEEM, e.g. a layer that is very thin there but thicker at most ~~positions~~ sites would be considered thin. To overcome this, we calculate the mean shifts applied to the values that were aligned and thus averaged. On average, i.e. for constant accumulation rates, we would expect these shifts to go linear with depth for the layering to be representative. Thus we calculate a linear least squares regression and correct the depth ~~scale~~ accordingly.

Nonetheless, the depth scale still represents the accumulation rate at NEEM. To transfer the average profile to any location X in the sampling area of known accumulation (not necessarily one of the N2E sites), we need to calculate a linear rescaling

factor f_X for the depth d_X that fulfills

$$d_{NEEM} = d_X \cdot f_X. \quad (6)$$

We expect f_X to be determined by the accumulation rate, or rather its ratio to the one at NEEM.

3.2 Significance testing and surrogate density profiles

- 5 Any alignment method will increase the covariance between records even if they are not related (Haam and Huybers, 2010). Therefore, to test the statistical significance of our density alignment, we generate sets of surrogate density profiles with similar statistical properties ~~for each position independently for each site~~ and process them the same way as the ~~real data-original data~~. Alongside the artificial density profiles, the real $\delta^{18}\text{O}$ signals are used for the coarse fitting step.

The complexity of the density signal consisting of slow variations, sharp ~~layer-property~~ changes as well as strong melt layer and wind crust related density spikes inhibits the use of simple surrogate construction methods such as autoregressive processes. Instead we propose the following algorithm.

- As For each site, as a base curve, we identify the $\delta^{18}\text{O}$ component of the density signal by linear regression, using the same step size l_{low} as for the coarse ($\delta^{18}\text{O}$ based) fitting step. This can be done because we rely on $\delta^{18}\text{O}$ to follow a seasonal cycle – otherwise water isotope dating would be impossible. Let ρ_{base} be the base density from $\delta^{18}\text{O}$, r_{low} the autocorrelation and σ_{base} the standard deviation of the fluctuations of the measured density (averaged to resolution l_{low}) around ρ_{base} for lag l_{low} . We start generating an artificial low resolution density profile ρ_{low} by

$$\rho_{low}(\underline{x}z_i) = \rho_{base}(\underline{x}z_i) + \varepsilon_i \quad (7)$$

$$\varepsilon_i = \begin{cases} \nu_0 & \text{for } i = 0 \\ r_{low} \cdot \varepsilon_{i-1} + \nu_i & \text{else} \end{cases} \quad (8)$$

$$\nu \sim \mathcal{N}(0, \sigma_{base}) \quad (9)$$

- 20 where $\underline{x}z_i = \underline{x}z_0 + i \cdot l_{low}$. (10)

Here $\nu \sim \mathcal{N}(0, \sigma_{base})$ implies that the ν_i are distributed normally with mean ~~0-zero~~ and standard deviation σ_{base} . In the following, $\mathcal{U}(0, 1)$ will represent a continuous uniform distribution for the interval $[0, 1]$. The inclusion of higher autocorrelation lengths is ~~straightforwardstraightforward~~. r_{low} has to be replaced by the autocorrelation matrix, which is multiplied with a vector of the preceding ε_i . Second, on the fine scale (step size l_{high}), we have a look at the differences between the interpolated low resolution density and the ~~high-resolution density values in-high-resolution density values from~~ the measurements. As we find the distribution to be trimodal, we split the differences in three components - low amplitude variations within ~~the same-layer snow of similar properties~~ (henceforth denoted "noise" even though they might partly have physical origin), fast and moderate amplitude changes in the density ~~at layer-transitions due to layering~~ or wind crusts ("shocks") and rapid high amplitude changes at melt layers ("melt"). Again, we compute the autocorrelation factor r_{high} for lag l_{high} . Nonetheless, this time, the standard deviations σ_{noise} , σ_{shocks} and σ_{melt} and the means μ_{shocks} and μ_{melt} have to be calculated separately.

Furthermore we need to estimate the probabilities P_{shocks} and P_{melt} of beginning a shock or a melt layer at a specific position. For this purpose, we determine the number of melt layers N_{melt} , the number of shocks N_{shocks} and the average distance to the previous shock d_{avg} . In addition, we denote the total number of data points by N and the distance to the last shock at a given position i by d_i . Finally, the basic model to generate a random density profile ρ_{high} is

$$5 \quad \rho_{high}(\underline{xz}_i) = \rho_{low}(\underline{xz}_i) + \kappa_i \quad (11)$$

$$\kappa_i = \begin{cases} \phi_i & \text{for } i = 0 \text{ or } P > P_{melt} + P_{shocks} \\ \mathcal{N}(\mu_{shocks}, \sigma_{shocks}) & \text{for } i \neq 0 \text{ and } P_{melt} < P \leq P_{melt} + P_{shocks} \\ \mathcal{N}(\mu_{melt}, \sigma_{melt}) & \text{for } i \neq 0 \text{ and } P \leq P_{melt} \end{cases} \quad (12)$$

$$P_{melt} = \frac{N_{melt}}{N} \quad (13)$$

$$P_{shocks} = \frac{d_i}{d_{avg}} \cdot \frac{N_{shocks}}{N} \quad (14)$$

$$P \sim \mathcal{U}(0, 1) \quad (15)$$

$$10 \quad \phi_i = \begin{cases} \nu_0 & \text{for } i = 0 \\ r_{high} \cdot \phi_{i-1} + \nu_i & \text{else} \end{cases} \quad (16)$$

$$\nu \sim \mathcal{N}(0, \sigma_{base}) \quad (17)$$

$$\text{where } \underline{xz}_i = \underline{xz}_0 + i \cdot l_{high}. \quad (18)$$

The same approach as before can be used to expand to higher autocorrelation lengths. However, we use the model in the presented form as it already provides realistic density surrogates.

15 4 Results

4.1 Profile alignment

As an example of the matching process, we present a fit of data from N2E_11 to the first position-site (NEEM) in Fig. 4. The distance between the two locations is approximately about 240 km, i.e. a little more than half of the total traverse length. First the $\delta^{18}\text{O}$ profiles are matched, yielding an approximately linearly increasing coarse shift. In the second step the densities are fine-tuned fine-tuned, which results in small shifts fluctuating around zero and never reaching the allowed maximum of 0.1 m. To provide an overview of the changing snow structure, we fit-fitted all combinations of two liners-profiles from two sites and plotted the matrix of the root mean square errors (RMSE) of in Fig. 5. A noticeable-remarkable change in the pattern of the fitting errors occurs between the fourth and fifth position-site along the traverse.

Figure 6 shows the continuous depth scale-alignment obtained by fitting all liners along the traverse to the first position-site (NEEM). There were no notable differences when another location (e.g. EGRIP) was chosen as the reference or the fitting

was done consecutively. For comparison, the melt layer positions detected during the CT measurements (cf. Table 3) have been included. In addition, selected density profiles are displayed. Using the previously calculated depth scale-alignment, density records were stacked to obtain a representative density profile (Fig. 7). The gray area indicates a one standard deviation error band. Comparing the necessary rescaling factors (known from the construction of the stacked profile) to the ratio of
 5 accumulation rates, we apply linear least squares to find

$$f_X = 0.325 + 0.665 \cdot \frac{\dot{a}_{NEEM}}{\dot{a}_X} \quad (19)$$

where \dot{a}_X denotes the mean annual accumulation rate at position-site X . The coefficient of determination is $R^2 = 0.82$.

At the base resolution of 0.1 cm we find a mean shared variance of $R^2 = 0.56$ between the average and the individual density profiles. It can be increased by smoothing and obtains a maximum of $R^2 = 0.71$ when using a 4.3 cm moving average.
 10 In comparison, for 1000 randomly generated density data sets (e.g. Fig. 8), the respective stacked profiles share an average of $R^2 = 0.44$ with their components at base resolution. The maximum is $R^2 = 0.61$. We determine a p -value (probability of finding such high R^2 by chance) of 0.015 for the measured profiles within the distribution, i.e. the high shared variance of the measured profiles is statistically significant.

4.2 Raw densities, isotope extrema and accumulation rates

15 ~~All of the liners show~~ For all sites we find at least two melt layers in the snow isotopically dating back to the summer of 2012. In addition, some liners show melt layers which are surrounded by snow dating to winter 2011/2012 or summer 2011. For an overview of all melt layers see Table 3 or Fig. 6. From the raw density profiles, we obtain Fig. 9, that shows the average densities of the top meter and decimeter, which do not contain any prominent melt layers. The density in the top meter tends to decrease from the maximum of 332 kg m^{-3} at NEEM down to a minimum of 297 kg m^{-3} roughly 150 km from EGRIP before
 20 slightly increasing again. For 15 out of 18 positions-sites the surface density is higher, nonetheless both parameters evolve similarly along the traverse.

Table 3 displays the mean annual accumulation rates along the traverse. Starting with a maximum of $225 \text{ kg m}^{-2} \text{ a}^{-1}$ at NEEM the values steadily decrease down to the minimum of $115 \text{ kg m}^{-2} \text{ a}^{-1}$ about 100 km from EGRIP before slightly increasing again to $140 \text{ kg m}^{-2} \text{ a}^{-1}$ at EGRIP. Comparing average values for the different years there is neither a trend nor
 25 considerable variations in the accumulation rate (cf. Table 4). However, we observe much higher differences between successive years within the same core (average change $34.67 \text{ kg m}^{-2} \text{ a}^{-1}$), where we mainly see alternating behaviour-behavior of high and low accumulation years.

Of the five years contained in our data, 2012 had the isotopically warmest summer for 83% of the positions-sites. At the three remaining locations (N2E_11, N2E_16 and EGRIP), the highest $\delta^{18}\text{O}$ values occur in 2014. For the winters, 2014/15 was
 30 isotopically coldest in 51% of the cases, 2011/12 in 19% and 2010/11 in 30%. Regarding annual $\delta^{18}\text{O}$ averages of all available positions-sites (Table 4), we also find the highest $\delta^{18}\text{O}$ values for 2012.

4.3 Linking accumulation, $\delta^{18}\text{O}$ and density

Comparing the annual average $\delta^{18}\text{O}$ values with the accumulation rates we obtain Fig. 10. Positive linear relations were fit to the data of 2012, 2013 and 2014 respectively, showing that within one year higher temperatures coincide with higher accumulation. The coefficient of determination is highest for 2012, while we have ~~more outliers~~ larger spreads for the other two years, in particular 2013.

To relate the density with the seasonal, ~~low-frequency~~ low-frequency $\delta^{18}\text{O}$ signal at NEEM, we applied a 10 cm running mean to the stacked ~~high-resolution~~ high-resolution density profile in Fig. 11. On average, snow with a high $\delta^{18}\text{O}$ value (considered summer snow) has a low density and the other way around. The only exception is the summer of 2012, where we find high density values in summer, too.

5 Discussion

5.1 New methodology

The liner technique allows us to retrieve non-disturbed snow samples from the field and thereby conduct lab-based analysis (such as ~~high-resolution~~ high-resolution density measurements) to gain further insight in the development of physical snow properties over large distances. This is a major improvement compared to previous methods, e.g. for measuring snow density, which was so far mainly done by ~~weighting~~ weighing a known volume of snow where we have a trade-off of accuracy (bulk density) and resolution (density cutters). Both \bar{r} -horizontal resolution and vertical depth can be adjusted to fit the needs of the respective study.

Figure 4 illustrates that we are able to align $\delta^{18}\text{O}$ and density data down to small stratigraphic features very well over a distance of over 200 km. Along the traverse, one observes a clear change in the RMSE (cf. Fig. 5) and thereby the snow structure at the fourth ~~linersite~~ linersite, indicated by significantly different fitting errors. This coincides with the location where the ice divide was left eastwards and thereby the traverse entered a different accumulation regime in agreement with the drainage systems given by Zwally et al. (2011).

Furthermore the continuous depth ~~scale-alignment~~ scale-alignment agrees very well with the melt layer positions detected during the CT measurements (Fig. 6). Stratigraphic features are still well aligned over the complete traverse distance of almost 450 km. We obtain a clear picture of the layering of the snowpack along the traverse. In comparison to radar measurements, which are limited to centimeter vertical resolution but can resolve annual layers down to 12 m (Hawley et al., 2006), we can give a much more precise picture and observe ~~small-scale~~ small-scale structures like wind crusts. In exchange we are limited to shallower depths – the maximum we plan to access in the near future are six meters in a trench at the EGRIP drilling site.

For rescaling the stacked profile to a-any location in the area with known annual accumulation, we obtain a linear relation of the depth factor with the ratio of accumulation rates. This is plausible, because, on average, we find linearly increasing shifts for the matching. Furthermore we do not ~~expect significant compaction~~ observe significant densification in the upper two meters

of the snowpack and therefore the depth of snow from the same deposition event is primarily determined by the accumulation rate. In addition, the relation has a high coefficient of determination for the applied linear least squares.

As the stratigraphy does not seem to change ~~significantly~~ remarkably along the traverse apart from the effect of the decreasing accumulation rate, we consider the profile in Fig. 7 to be representative for the whole traverse region, potentially even most of North Greenland. For the given error band, there is an overlap of uncertainty in the depth alignment (x -direction) with the uncertainty in density (y -direction). The former is mainly caused by the variability of the snow mass accumulated from a single deposition event. Regarding the latter, the average density of the snowpack greatly varies as can be seen in Fig. 9. Thus, for the second meter, even though it is contained in the uncertainty band, we do not expect a straight line, but rather an alternation of high and low density layers similar to the upper meter.

A statistical test using surrogate density profiles shows that the high shared variance of the measured profiles is statistically significant ($p = 0.015$), even though the actual difference in numbers is quite small. This underlines that the density alignment provides additional information as we tried to use the most realistic surrogates (original $\delta^{18}\text{O}$ signal, seasonal cycle, three component stratigraphy model). Furthermore, a coefficient of determination of $R^2 = 0.56$ between the stacked and the individual profiles shows how much of the layering does reappear. Smoothing increases R^2 ~~up to 0.71~~ as it steadily transforms the profile to the low resolution density curve that shows seasonal ~~behaviour~~ behavior (see Fig. 11) while smaller local variations vanish.

5.2 Temporal and regional variability of snow properties

The vast majority of melt layers ~~is~~ are found in snow dating back to the very warm summer of 2012 (Nghiem et al., 2012). Moreover, above most of the melt layers within older snow, we find clear signs of percolation (cf. Fig. 2). Therefore we assume that 2012 was the only year in the period 2010–2015 with significant melt occurring in the observed area. From Fig. 9 we can infer that on the one hand the average density of the snow in the top two meters at a certain ~~position~~ location can already be deduced from the surface density. On the other hand the surface snow in May is among the denser ones within the year, thereby rather representing a spring or even winter signal than a ~~sommer~~ summer one (compare Fig. 11). Furthermore we are able to visually identify many layers of homogeneous density, often clearly separated by wind crusts, that ~~thereby~~ seem to contain snow from single deposition events.

For the accumulation rate (see Table 3) the 1964 – 2005 average of $220 \text{ kg m}^{-2} \text{ a}^{-1}$ determined from the NEEM ice core (Steen-Larsen et al., 2011) agrees very well with the $225 \text{ kg m}^{-2} \text{ a}^{-1}$ that we obtain from the corresponding snow liner. In addition, both, accumulation maps from field measurements (Bales et al., 2009) and regional climate models (Fettweis, 2007), show the same ~~behaviour~~ behavior towards the East. While Table 4 shows no significant interannual changes in the average accumulation rate for the study area, we observe high fluctuations in the local annual values, a feature consistent with the strong influence of stratigraphic noise in single profiles (Muench et al., 2015). These can be explained by the accumulation of every year compensating previous local variations in the snow surface before new structures are introduced by wind-induced drift and dunes. Nonetheless, they also might partly originate from the uncertainty of separating the years only according to the $\delta^{18}\text{O}$ extrema.

In the majority of cases we find the highest isotopic summer temperatures and average $\delta^{18}\text{O}$ values for 2012, underlining the exceptional warmth of this year. The values for 2014 indicate that it was still warmer than the other contained years, in particular 2010, which was formerly regarded as very warm (Harper et al., 2012). The picture for the winters is less clear. ~~Furthermore~~ Indeed, we assume that the isotopic signal of the fresh snow from winter 2014/15 might still change.

5 5.3 Relations of density, $\delta^{18}\text{O}$ and accumulation rate

We find a positive linear relationship of annual mean $\delta^{18}\text{O}$ and accumulation rate (Fig. 10) with similar slopes for 2012 and 2014. This relation might partly originate from the changing surrounding conditions (e.g. elevation) along the traverse. The offset between the years could potentially be caused by the very high temperatures and the consequential surface melting in 2012 as we find the relation for 2013 to be a lot closer to 2014 than 2012. The dependence of the offset on the annual mean temperature (which is quite similar along the traverse) could explain why previous attempts to link both parameters by averaging data from several years (e.g. Weißbach et al., 2016) show less clear results.

We observe a clear anticorrelation of low resolution density and $\delta^{18}\text{O}$ in Fig. 11. This agrees with the widely accepted conceptual model of Shimizu (1964) which states that snow has lower densities in summer and higher ones in winter. The ~~high average densities in summer~~ main causes given are the increased packing due to stronger winds in winter and the larger size of precipitation particles in summer. For the summer of 2012, the high average densities are caused by the prominent melt layers, superimposing the original ~~snow density signal~~ signal of the snow.

6 Summary and conclusions

We introduced the liner technique, that allows the very efficient retrieval of ~~high-quality~~ high-quality samples from the upper meters of the snowpack. To support this new sampling technique, we adapted a robust fitting algorithm from ~~aeoustic~~ acoustic signal processing for the diverse data sets produced by such studies. This enables us to identify characteristic changes in the snowpack according to surrounding conditions as well as to generate a continuous depth ~~scale~~ alignment using features from all available records.

To demonstrate their feasibility we applied the described methods to the upper two meters of snow along a traverse in North Greenland. We obtain a record up to May 2015 of the depths of the 2012 melt layers and ~~sub-millimeter resolution~~ sub-millimeter-resolution densities. By combining these with $\delta^{18}\text{O}$ measurements, that indicate temperature, we are able to reconstruct accurate accumulation rates for the years 2010 – 2014 along a distance of about 400 km.

We combine isotope and density data as inputs for the matching algorithm. Thereby we are able to identify the different accumulation regimes along the traverse and resolve the continuous stratigraphy of the snow over the whole distance. This allows us to create a representative density profile for the study area, whose quality is proven by comparison with randomly generated data based on a statistical density model. The profile is available at a resolution of 0.1 cm and only has to be rescaled according to accumulation rate. Thus it is ready to act as a benchmark for ~~model outputs~~ snowpack models or be applied for the

conversion of volume to mass [and the detection of strong density gradients as potential reflectors](#) in remote sensing (compare e.g. Hurkmans et al., 2014).

5 The success of fitting density and isotope profiles over hundreds of kilometers shows that even though there is a local component in the snow stratigraphy (e.g. layer thickness, average density) the general pattern is dominated by non-local processes in North Greenland. We assume that an important factor for that is the origin of weather and precipitation as air masses dominantly move in from the West to the East (Chen et al., 1997).

10 We observe large interannual accumulation variations locally but almost none on average, which can be explained by the smoothing of the surface by accumulation before new surface structures are caused by dunes and drift. The exceptionally warm summer [of](#) 2012 is clearly visible in the water isotope data, additionally 2014 shows the second highest summer values of $\delta^{18}\text{O}$ within the study period.

15 Relating the various snow properties we find a distinct anticorrelation of smoothed density and $\delta^{18}\text{O}$ in accordance with previous literature. Furthermore we deduce a positive linear relation between $\delta^{18}\text{O}$ and accumulation rate, whose slope seems to be constant for the period considered while the offset varies between the years and thus might be temperature-dependent. This, however, poses the question whether models commonly used in the dating of deep ice cores (e.g. Parrenin et al., 2007, for the EPICA Dome C ice core) do correctly reconstruct accumulation rates from the $\delta^{18}\text{O}$ values, especially for times with significantly differing annual mean temperatures such as glacials.

Future work should include the automatic recognition of wind crusts and layering from CT images and the application of the described methods on different scales for both Antarctica and Greenland to gain further insight into the variability of physical properties in the snowpack.

20 *Author contributions.* Sepp Kipfstuhl took the samples and initiated the analysis process. Hans Christian Steen-Larsen was involved in the field planning and helped interpret the results with his expertise in the Greenland snowpack. Johannes Freitag originally established the CT method, supervised and evaluated the isotope measurements and regularly discussed preliminary results with the main author. Olaf Eisen helped relating the results to the literature and provided insights on alternative methods. Thomas Laepple recommended underlining the results with randomly generated data and suggested possible approaches. Christoph Schaller coordinated the CT measurements, evaluated
25 and analyzed the combined data and prepared this manuscript. It was reviewed by all coauthors.

Acknowledgements. The main author wants to thank the German National Merit Foundation (Studienstiftung des deutschen Volkes e.V.) for funding his PhD project, York Schlomann for conducting the isotope measurements and the involved CIC employees for organizing and supporting the traverse.

References

- Bales, R. C., Guo, Q., Shen, D., McConnell, J. R., Du, G., Burkhart, J. F., Spikes, V. B., Hanna, E., and Cappelen, J.: Annual accumulation for Greenland updated using ice core data developed during 2000–2006 and analysis of daily coastal meteorological data, *J. Geophys. Res.*, 114, D06 116, doi:10.1029/2008JD011208, 2009.
- 5 Bennartz, R., Shupe, M. D., Turner, D. D., Walden, V. P., Steffen, K., Cox, C. J., Kulie, M. S., Miller, N. B., and Pettersen, C.: July 2012 Greenland melt extent enhanced by low-level liquid clouds, *Nature*, 496, 83–86, doi:10.1038/nature12002, 2013.
- Benson, C. S.: Stratigraphic studies in the snow and firn of the Greenland Ice sheet, *USA SIPRE Res. Rep.*, 70, 1–89, 1962.
- Bull, C.: Snow Accumulation in North Greenland, *J. Glaciol.*, 3, 237–248, 1958.
- Chen, Q.-S., Bromwich, D. H., and Bai, L.: Precipitation over Greenland Retrieved by a Dynamic Method and Its Relation to Cyclonic Activity, *J. Climate*, 10, 839–870, 1997.
- 10 Fettweis, X.: Reconstruction of the 1979–2006 Greenland ice sheet surface mass balance using the regional climate model MAR, *The Cryosphere*, 1, 21–40, 2007.
- Fisher, D. A., Reeh, N., and Clausen, H. B.: Stratigraphic noise in the time series derived from ice cores, *Ann. Glaciol.*, 7, 76–83, 1985.
- Freitag, J., Kipfstuhl, S., and Laepple, T.: Core-scale radiosopic imaging: a new method reveals density-calcium link in Antarctic firn, *J. Glaciol.*, 59, 1009–1014, 2013.
- 15 Haam, E. and Huybers, P.: A test for the presence of covariance between time-uncertain series of data with application to the Dongge Cave speleothem and atmospheric radiocarbon records, *Paleoceanography*, 25, PA2209, doi:10.1029/2008PA001713, 2010.
- Hagenmuller, P. and Pilloix, T.: A New Method for Comparing and Matching Snow Profiles, Application for Profiles Measured by Penetrometers, *Front. Earth Sci.*, 4, doi:10.3389/feart.2016.00052, <http://journal.frontiersin.org/Article/10.3389/feart.2016.00052/abstract>, 2016.
- 20 Hanna, E., Huybrechts, P., Cappelen, J., Steffen, K., Bales, R. C., Burgess, E., McConnell, J. R., Steffensen, J. P., Van den Broeke, M., Wake, L., Bigg, G., Griffiths, M., and Savas, D.: Greenland Ice Sheet surface mass balance 1870 to 2010 based on Twentieth Century Reanalysis, and links with global climate forcing, *J. Geophys. Res.*, 116, D24 121, doi:10.1029/2011JD016387, 2011.
- Harper, J., Humphrey, N., Pfeffer, W. T., Brown, J., and Fettweis, X.: Greenland ice-sheet contribution to sea-level rise buffered by meltwater storage in firn, *Nature*, 491, 240–243, doi:10.1038/nature11566, 2012.
- 25 Hawley, R. L., Morris, E. M., Cullen, R., Nixdorf, U., Shepherd, A. P., and Wingham, D. J.: ASIRAS airborne radar resolves internal annual layers in the dry-snow zone of Greenland, *Geophys. Res. Lett.*, 33, L04 502, doi:10.1029/2005GL025147, 2006.
- Hawley, R. L., Courville, Z. R., Kehrl, L. M., Lutz, E. R., Osterberg, E. C., Overly, T. B., and Wong, G. J.: Recent accumulation variability in northwest Greenland from ground-penetrating radar and shallow cores along the Greenland Inland Traverse, *J. Glaciol.*, 60, 375–382, doi:10.3189/2014JoG13J141, 2014.
- 30 Hurkmans, R. T. W. L., Bamber, J. L., Davis, C. H., Joughin, I. R., Khvorostovsky, K. S., Smith, B. S., and Schoen, N.: Time-evolving mass loss of the Greenland Ice Sheet from satellite altimetry, *The Cryosphere*, 8, 1725–1740, doi:10.5194/tc-8-1725-2014, 2014.
- Itakura, F.: Minimum prediction residual principle applied to speech recognition, *IEEE T. Acoust. Speech*, 23, 67–72, 1975.
- Koenig, L. S., Ivanoff, A., Alexander, P. M., MacGregor, J. A., Fettweis, X., Panzer, B., Paden, J. D., Forster, R. R., Das, I., McConnell, J., Tedesco, M., Leuschen, C., and Gogineni, P.: Annual Greenland accumulation rates (2009–2012) from airborne Snow Radar, *The Cryosphere Discussions*, 9, 6697–6731, doi:10.5194/tcd-9-6697-2015, 2015.
- 35 Lenton, T. M., Held, H., Kriegler, E., Hall, J. W., Lucht, W., Rahmstorf, S., and Schellnhuber, H. J.: Tipping elements in the Earth’s climate system, *P. Natl. Acad. Sci. USA*, 105, 1786–1793, 2008.

- McConnell, R., Kwok, R., Curlander, J., Kober, W., and Pang, S.: psi-s correlation and dynamic time warping: two methods for tracking ice floes in SAR images, *IEEE T. Geosci. Remote*, 29, 1004–1012, doi:10.1109/36.101377, <http://ieeexplore.ieee.org/lpdocs/epic03/wrapper.htm?arnumber=101377>, 1991.
- Muench, T., Kipfstuhl, S., Freitag, J., Meyer, H., and Laepple, T.: Regional climate signal vs. local noise: a two-dimensional view of water isotopes in Antarctic firn at Kohnen station, Dronning Maud Land, *Clim. Past Discussions*, 11, 5605–5649, doi:10.5194/cpd-11-5605-2015, 2015.
- Nghiem, S. V., Hall, D. K., Mote, T. L., Tedesco, M., Albert, M. R., Keegan, K., Shuman, C. A., DiGirolamo, N. E., and Neumann, G.: The extreme melt across the Greenland ice sheet in 2012, *Geophys. Res. Lett.*, 39, L20 502, doi:10.1029/2012GL053611, 2012.
- Nilsson, J., Vallenga, P., Simonsen, S. B., Sorensen, L. S., Forsberg, R., Dahl-Jensen, D., Hirabayashi, M., Goto-Azuma, K., Hvidberg, C. S., Kjaer, H. A., and Satow, K.: Greenland 2012 melt event effects on CryoSat-2 radar altimetry, *Geophys. Res. Lett.*, 42, 3919–3926, doi:10.1002/2015GL063296, 2015.
- Parrenin, F., Barnola, J.-M., Beer, J., Blunier, T., Castellano, E., Chappellaz, J., Dreyfus, G., Fischer, H., Fujita, S., Jouzel, J., and others: The EDC3 chronology for the EPICA Dome C ice core, *Clim. Past*, 3, 485–497, 2007.
- Sakoe, H. and Chiba, S.: Dynamic programming algorithm optimization for spoken word recognition, *IEEE T. Acoust. Speech*, 26, 43–49, doi:10.1109/TASSP.1978.1163055, 1978.
- Sakurai, Y., Faloutsos, C., and Yamamuro, M.: Stream monitoring under the time warping distance, *Proc. Int. Conf. Data*, pp. 1046–1055, doi:10.1109/ICDE.2007.368963, 2007.
- Senin, P.: Dynamic time warping algorithm review, Tech. rep., University of Hawaii, Honolulu, USA, 2008.
- Shimizu, H.: Glaciological Studies in West Antarctica 1960–1962, in: *Antarct. Res. Ser.*, edited by Mellor, M., pp. 37–64, American Geophysical Union, Washington, D. C., 1964.
- Steen-Larsen, H. C., Masson-Delmotte, V., Sjolte, J., Johnsen, S. J., Vinther, B. M., Breon, F.-M., Clausen, H. B., Dahl-Jensen, D., Falourd, S., Fettweis, X., Galée, H., Jouzel, J., Kageyama, M., Lerche, H., Minster, B., Picard, G., Punge, H. J., Risi, C., Salas, D., Schwander, J., Steffen, K., Sveinbjornsdottir, A. E., Svensson, A., and White, J.: Understanding the climatic signal in the water stable isotope records from the NEEM shallow firn/ice cores in northwest Greenland, *J. Geophys. Res.*, 116, D06 108, doi:10.1029/2010JD014311, 2011.
- Weißbach, S., Wegner, A., Opel, T., Oerter, H., Vinther, B. M., and Kipfstuhl, S.: Spatial and temporal oxygen isotope variability in northern Greenland – implications for a new climate record over the past millennium, *Clim. Past*, 12, 171–188, doi:10.5194/cp-12-171-2016, 2016.
- Zwally, H. J., Jun, L. I., Brenner, A. C., Beckley, M., Cornejo, H. G., DiMarzio, J., Giovinetto, M. B., Neumann, T. A., Robbins, J., Saba, J. L., and others: Greenland ice sheet mass balance: distribution of increased mass loss with climate warming; 2003–07 versus 1992–2002, *J. Glaciol.*, 57, 88–102, 2011.

Table 1. Measurement ~~positions~~sites along the traverse, see also Fig. 1. The missing liner numbers (e.g. N2E_01) result from multiple samples being taken at some locations. Nonetheless, only one profile per ~~position~~location was used for this study.

Position <u>Site</u>	Longitude	Latitude	Traverse kilometer
NEEM (N2E_02)	51.06914° W	77.444337° N	0.00
N2E_03	50.11° W	77.3669° N	24.80
N2E_04	49.23077° W	77.25429° N	49.66
N2E_05	48.170872° W	77.120098° N	79.76
N2E_06	47.13806° W	76.98195° N	109.73
N2E_07	46.14227° W	76.84788° N	138.90
N2E_08	45.27375° W	76.71337° N	165.57
N2E_09	44.78786° W	76.52426° N	190.03
N2E_10	44.09225° W	76.40034° N	212.78
N2E_11	43.06116° W	76.32535° N	241.07
N2E_12	42.051636° W	76.248888° N	269.01
N2E_14	41.16026° W	76.1777° N	293.92
N2E_15	40.29929° W	76.10455° N	318.25
N2E_16	39.31873° W	76.01559° N	346.32
N2E_17	38.46937° W	75.93539° N	370.88
N2E_19	37.69747° W	75.85845° N	393.48
N2E_20	36.54374° W	75.70614° N	429.25
EGRIP (N2E_22)	35.985618° W	75.629343° N	446.83

Table 2. Fitting parameters for our adaption of the DTW algorithm.

Property (step)	Step size (l)	Maximal <u>Maximum</u> surface offset (s)	Maximal <u>Maximum</u> bottom offset (b)
$\delta^{18}\text{O}$ (coarse)	3 cm	15 cm	75 cm
Density (fine)	0.1 cm	10 cm	10 cm

Table 3. Melt layers, the water isotopic season of origin for the surrounding snow and mean annual accumulation rates for each [position site](#). The given depths indicate the vertical center of the respective melt layer. The upper two melt layers are always located in snow from summer 2012. For the lower ones, the season of origin for the surrounding snow is given, where S indicates summer and W winter. The accumulation rates are annual mean values for all available years at the particular [position location](#).

Position Site	Depth 1 [m]	Depth 2 [m]	Depth 3 [m]	Snow origin	Depth 4 [m]	Snow origin	Accumulation [$\text{kg m}^{-2} \text{a}^{-1}$]
NEEM	1.76	1.84					224.69
N2E_03	1.61	1.68	1.76	S2012			193.8
N2E_04	1.47	1.60	1.77	W11/12	1.87	W11/12	205.04
N2E_05	1.35	1.54	1.67	W11/12			171.55
N2E_06	1.48	1.67					193.46
N2E_07	1.37	1.50					165.38
N2E_08	1.37	1.41					162.67
N2E_09	1.33	1.42					155.85
N2E_10	1.31	1.39					135.01
N2E_11	1.21	1.36	1.50	W11/12			137.58
N2E_12	1.15	1.21					124.73
N2E_14	1.12	1.18					117.30
N2E_15	1.10	1.20					126.78
N2E_16	1.13	1.16	1.33	W11/12			115.06
N2E_17	1.19	1.23	1.50	W11/12			129.88
N2E_19	1.13	1.17	1.42	S2011			132.16
N2E_20	1.35	1.41	1.48	W11/12	1.61	S2011	145.93
EGRIP	1.22	1.32	1.57	W11/12			139.57

Table 4. Mean deviations of the given year from the average local annual ([winter to winter](#)[winter-to-winter](#)) accumulation rate and $\delta^{18}\text{O}$. For each year, data from all available sites were used.

Year	\dot{a} anomaly [$\text{kg m}^{-2} \text{a}^{-1}$]	$\delta^{18}\text{O}$ anomaly [‰]	Unavailable position sites
2014	-2.66	-0.88	-
2013	5.26	-1.25	-
2012	3.20	3.64	NEEM, N2E_06
2011	-7.37	-2.31	NEEM, N2E_03-N2E03 – N2E_09

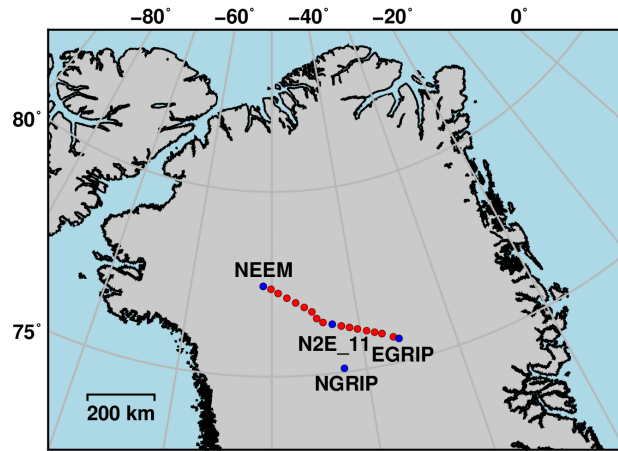


Figure 1. The N2E traverse route with the measurement positions sites according to Table 1.

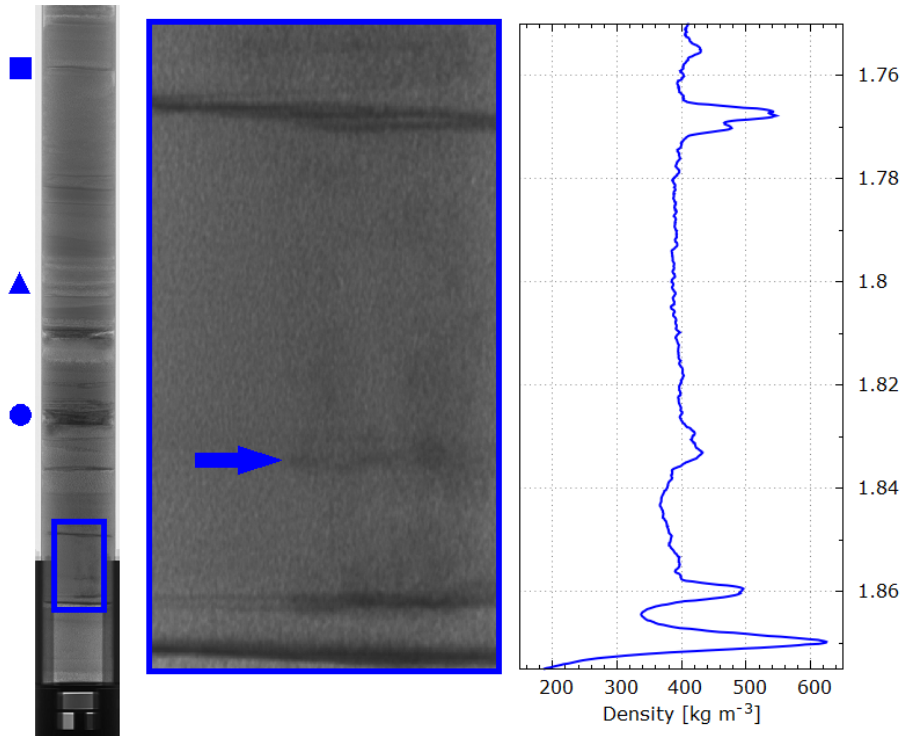


Figure 2. Example 2D CT image of a one meter liner (depth: 1 – 2 m depth) and a zoomed section showing two melt layers aligned with the respective densities. In the left image a distinct density layering (e.g. blue triangle), several melt layers (e.g. blue circle) and wind crusts (e.g. blue square) are visible. Above the lower zoomed melt layer a clear percolation pattern (blue arrow) can be seen on the right hand side of the snow core.

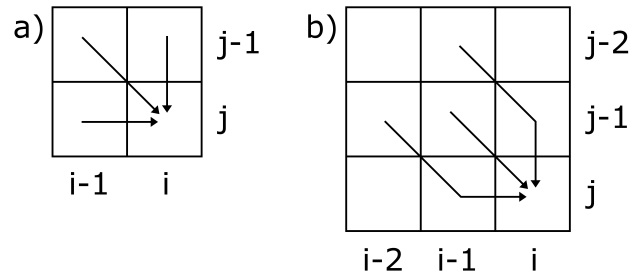


Figure 3. a) Basic and b) constrained stepping patterns for the DTW algorithm. Usage of cell $[i, j]$ indicates that the i 'th element of the first and the j 'th element of the second data set were matched. The basic pattern allows for a single value to be assigned to arbitrarily many of the other data set, while for the constrained stepping each value can only be ~~matched~~ identified with one or two others.

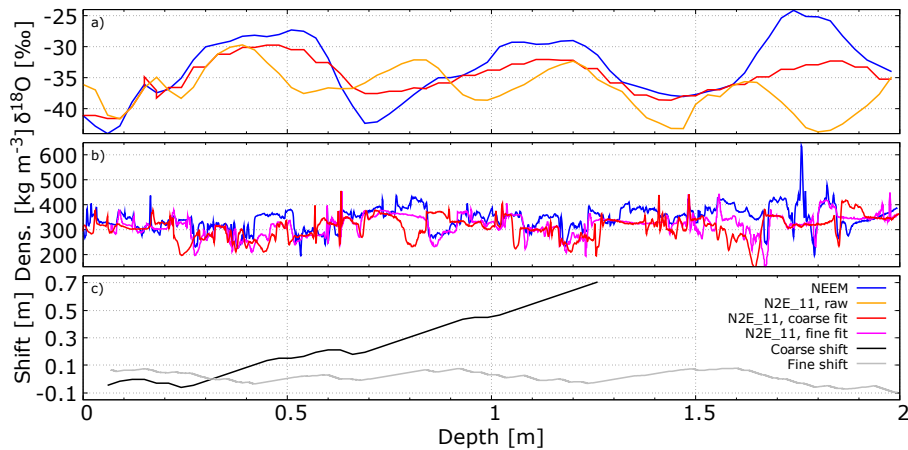


Figure 4. Alignment of the data from NEEM and N2E_11. a) First, the raw $\delta^{18}\text{O}$ data from N2E_11 (orange) are fit to those of NEEM (blue) resulting in the red curve. b) Then, the calculated (coarse) shifts are applied to the raw N2E_11 density data to obtain the red curve as an input for a second alignment with the raw NEEM density profile (blue). We end up with the pink curve as a final result. c) The applied coarse (black) and fine (gray) shifts.

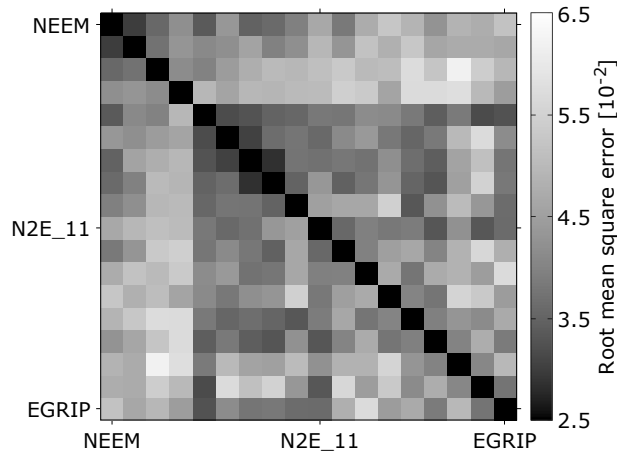


Figure 5. Root mean square matrix of the density alignment. The n 'th field in the m 'th row refers to the error of fitting data from the n 'th and m 'th liner. The darker the color, the lower the error and therefore the higher the agreement. Between~~The most notable change in snow structure can be observed between~~ the fourth and the fifth column (or row)~~a notable change in snow structure can be observed.~~

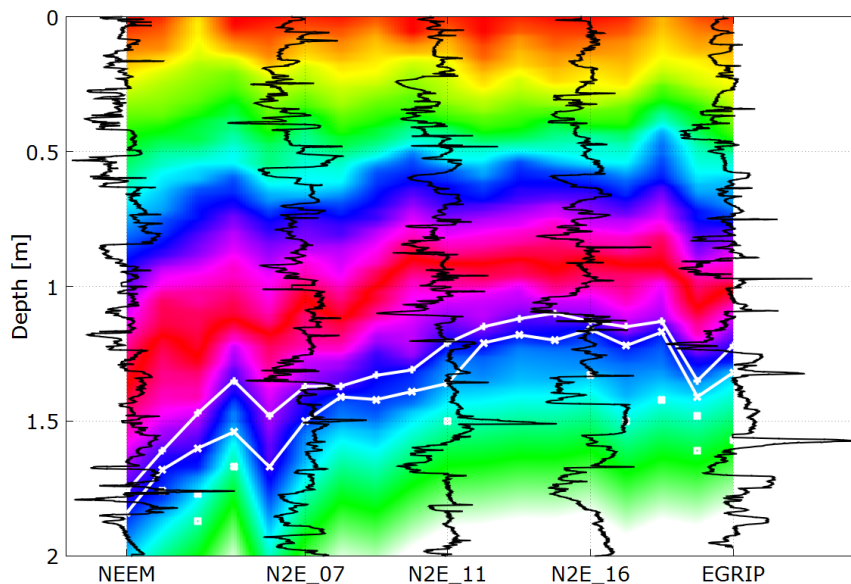


Figure 6. Moving-Continuous depth scale alignment, example density profiles and melt layers. A colormap was applied uniformly at the first position-site (NEEM) and then transformed the same way as the depths were aligned assigned. Thus snow within the same color band was matched during the fitting process. Measured-Linear interpolation was used between the sampled sites. In black, measured density profiles for the labeled positions-locations are shown in-black at the same scale, centered around their respective mean values. The white lines and points indicate the melt layer positions detected from the CT scans (cf. Table 3).

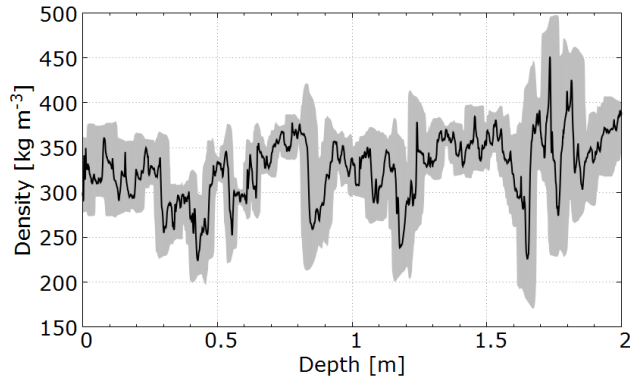


Figure 7. Representative density profile for the traverse region. The gray area indicates a one standard deviation error band in both x - and y -direction as there are uncertainties in the depth alignment as well as the averaged densities of all [position sites](#). Here, the depth scale was adjusted to the NEEM accumulation rate and has to be rescaled according to accumulation rate for different sites.

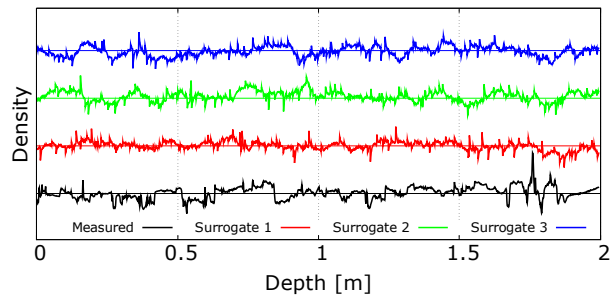


Figure 8. The measured density profile and three surrogates for the first [position site](#) (NEEM). The [random artificial](#) profiles are based on the seasonal $\delta^{18}\text{O}$ component of the density and have the same statistical properties as the original curve. [Each profile is displayed at the same scale and has been centered around its mean.](#)

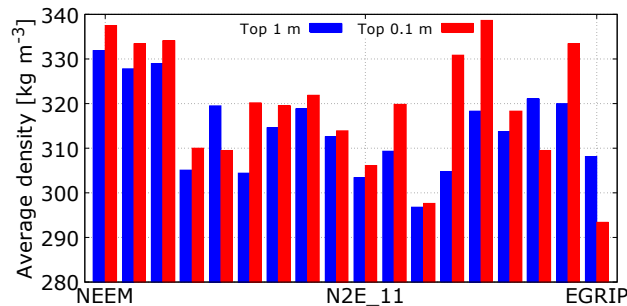


Figure 9. Average densities along the traverse through North Greenland (May 2015) in the top 1 m and 0.1 m derived from CT data.

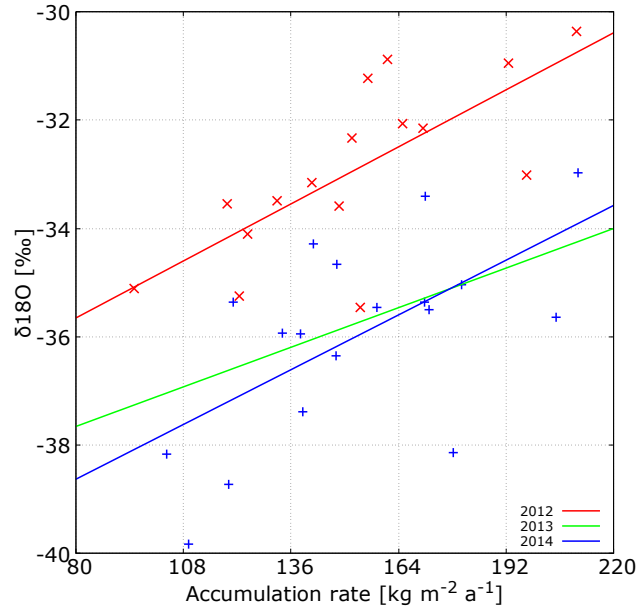


Figure 10. $\delta^{18}\text{O}$ signal versus accumulation rate for the years 2012 – 2014. The lines were obtained by linear least squares fitting with coefficients of determination of $R^2 = 0.52$ for 2012, $R^2 = 0.27$ for 2013 and $R^2 = 0.37$ for 2014. The data points for 2013 show ~~a few outliers~~ the largest spread and were omitted for clarity.

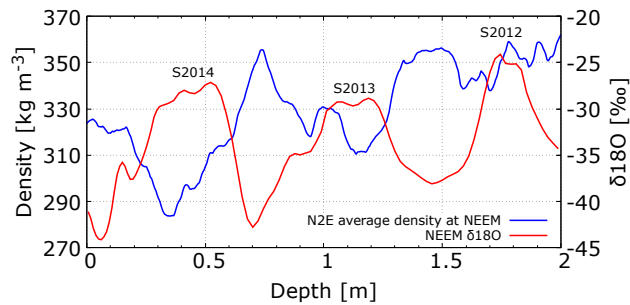


Figure 11. Comparison of the NEEM $\delta^{18}\text{O}$ signal with the stacked density profile on the NEEM ~~depthscale~~ depth scale smoothed using 10 cm running means. The summer maxima for 2012 – 2014 ~~are~~ were marked.